A Novel Wireless Local Positioning System via a Merger of DS-CDMA and Beamforming: Probability-of-Detection Performance Analysis under Array Perturbations

Hui Tong and Seyed A. Zekavat

Dept. of ECE, Michigan Tech. University, Houghton, MI, 49931

Phone: 906-487-1944, 906-487-2071, e-mail: htong@mtu.edu, rezaz@mtu.edu

Abstract

This Paper[1] investigates the Probability-of-Detection (POD) performance of a novel Wireless Local Positioning System (WLPS[2]) realized via Direct Sequence Code Division Multiple Access (DS-CDMA) and beamforming techniques. The proposed WLPS has unique signaling schemes that discriminate it from the traditional wireless systems and allows the WLPS to have many civilian and military applications. The WLPS consists of two main parts: (1) the detecting unit, a base station carried by a mobile unit defined as Dynamic Base Station (DBS), and (2) the being detected unit, a transponder (TRX) that is mounted on the targets, each assigned a unique identification code (ID code). Each DBS should be capable of detecting and locating all available TRXs in its coverage area. As a result, the main complexity of this system is focused at the DBS receiver.

In this work, we introduce WLPS structure, and both theoretically and numerically compute, and compare the Probability-of-Detection performance of the DBS receiver realized by a merger of DS-CDMA and antenna arrays. We also analyze and simulate the performance of this system under perturbations in the DBS antenna array vector. The simulations are particularly performed for vehicular collision avoidance applications.

This work is supported by the US NSF grant ECS-0427430

[1]Portions of this paper were previously reported in [1]–[3].

[2]The WLPS US Patent is pending by Michigan Tech. University.

Index Terms

Wireless Local Positioning System, DS-CDMA, Beamforming, perturbation analysis, vehicle collision avoidance.

I. INTRODUCTION

Historically, positioning was developed for navigational purposes with a wide variety of civilian and military applications, and they fall into two main categories, Global Positioning Systems (GPS) and Local Positioning Systems (LPS) [4]–[6]. GPS is a precise, all-weather, 24 hour satellite based positioning system mainly developed for direction finding and navigation [7]. However, GPS has the following problems: (1) its signal does not penetrate into the buildings; hence, it does not perform at indoor areas, (2) it looses its precision in rich scattering environments such as urban areas, (3) it is mainly suitable for navigation and for tracking or command purposes, it should be merged with a communication system for transmission of position information from the GPS to a center (e.g., command center in defense applications), and (4) it is yet expensive.

Local positioning systems (LPS) fall primarily into two main categories [8]: (1) Self Positioning: A mobile device finds its own instantaneous location with respect to a fixed point, e.g., the starting point or a beacon node, and (2) Remote Positioning: A mobile device finds the instantaneous positions of other objects (mobiles) with respect to its own position. The Wireless Local Positioning System (WLPS) introduced in this paper is a remote positioning system with active targets capable of detecting and locating targets within several hundred meters in a dynamic environment [1]–[3].

In the quest for wireless positioning, different systems have been developed or are under development. For example, radar systems are used to find the position of targets in the surrounding areas via transmission of a short burst of energy and processing its reflection from the targets [9] [10]. The ability of radars to detect the desired targets is hindered by clutters or reflections from undesirable objects and interfering radars, which are inevitable in typical indoor and urban areas, rendering radar systems impractical [11] [1]. Another example is a vision system that

uses video signals collected from a camera to recognize targets and estimate positions [12]. Such systems, including Chrysler's mobile positioning system, face major limitations at night and in severe weather conditions such as intense rain, snow and fog.

The Wireless Local Positioning System (WLPS) introduced in this paper consists of: (1) a base station in each monitoring mobile, which serves as a non-static or Dynamic Base Station (DBS), and (2) a transponder (TRX) in target mobiles, which acts as active targets. Unique IDentification (ID) codes are assigned to each target. DBS transmits a short pulse containing an ID Request (IDR) signal to all targets located in its vicinity, and it does not transmit within two consecutive IDRs called ID request Repetition Time (IRT). The targets respond to that signal by transmitting their ID codes back to the DBS. DBS recognizes each target by its ID code, and then positions, tracks and monitors those targets. Positioning is realized via calculating the Time-of-Arrival (TOA) and the Direction-of-Arrival (DOA). TOA is defined as the time difference between transmission of the ID request signal and reception of the corresponding TRX ID.

The performance of WLPS system depends on two main variables: a) Probability-of-Detection (POD) of the ID of each TRX, and b) accuracy of positioning, which is a function of the estimation of TOA and DOA. Both of these parameters are critical for the performance of WLPS system. In this paper, we focus on the Probability-of-Detection performance of the WLPS. The positioning performance of WLPS primarily depends on the development of DOA estimation techniques. These techniques that are unique for WLPS signaling method will be addressed in our future studies.

Many local positioning systems via active targets have been introduced in the literature. Examples include: (1) Airborne traffic alert and collision avoidance (TCAS) systems [13] [14] developed for future air navigation systems (FANS) [15] use transponders at airplanes (active targets) for positioning purposes. These systems use the radar principles for range resolution with a range of 10-40 miles [16] which leads to a limited capacity suitable for those applications. The technique used in TCAS is not feasible for wireless channels, which experience multi-path fading and interference effects, and cover a range of 0.1-1 mile in many applications; (2) Cell

phone positioning systems may exploit a triangulation technique [17] to estimate subscriber's position. In order to achieve a reasonable positioning accuracy (around $100m$), the subscriber's signal can be received by at least three base stations. But, this number of base stations might not be available at all times. In addition, experimental results show that the capability of this system is limited by multipath environments [18]. A merger of area power intensity map and directional antennas may also be utilized for cell phone positioning purposes [19]. This approach requires detailed information that constrains to static (as opposed to dynamic) positioning; (3) In tagged local positioning systems (TLPS), mobiles (active targets) transmit periodic signals at all times, and static base stations receive those signals and locate the targets via a triangulation technique [6]. In order to increase its robustness to multipath effects and increase its accuracy, this system utilizes additional readers and reference tags. These systems are limited to a relatively fixed environment [20]; and (4) In WLAN positioning systems, a triangulation technique is used by mobile nodes for positioning purposes. In order to perform triangulation, WLAN positioning requires a number of nodes to be involved in the positioning process [21]. Hence, positioning process can not be performed independently by each node, which limits the applications of these positioning systems.

In the WLPS introduced in this paper, each DBS is capable of positioning all TRXs in its coverage area. Moreover, the DBS does not need additional prior environmental information. Hence, WLPS is not limited to the fixed base station. In addition, via the application of wireless signaling schemes such as Code Division Multiple Access (CDMA), diversity combining and beamforming, the interference and multipath fading effects can be reduced and the probability of detection increases. The WLPS can be defined as a node in Mobile Adhoc Network (MANET) with a variety of applications in security systems (e.g., in indoor security via implementation of DBS and TRX on security guards and just TRX on people entering the building), vehicle collision avoidance system and multi robot control (e.g., by implementing the DBS and TRX on all vehicles or robots [1]), and defense (e.g., for command control and tracking, by implementation of DBS on the central command and control, DBS and TRX on all commanders and TRX on soldiers). The coverage area of WLPS can be increased via multiple-hop localization

techniques [2] [22] [23].

In this work, we investigate the realization of this system via standard transmitters and receivers (i.e., simple modulators and demodulators) as well as Direct Sequence CDMA (DS-CDMA) receivers with and without antenna arrays and beamforming (BF) techniques, and we compare their Probability-Of-Detection, P_d, performance. In DS-CDMA the transmitted symbol is multiplied in a spreading code in the time domain. Orthogonal spreading codes maintain the orthogonality between the signals transmitted from different TRXes. In addition, multipath fading effects are reduced by exploiting path diversity at the DS-CDMA receiver. This technique alone enhances the Probability-of-Detection (POD) performance of the DBS receiver. A merger of DS-CDMA with Spatial Division Multiple Access (SDMA) highly enhances the performance of the DBS. SDMA is accomplished by employing directionality via antenna arrays at the DBS receiver. These antenna arrays are required for DOA estimation as well. Our simulation depicts that by a proper selection of IRT, both DS-CDMA and standard Rake receivers with conventional BF lead to a high POD performance. Here, we particularly perform the simulations for vehicular collision avoidance (road safety) applications of WLPS.

In real applications, perturbation of the array weight vector due to effects such as sensor position errors, gain errors, phase errors, mutual coupling between sensors, imperfect channel phase estimation, and different cable length for each sensor degrades the receiver performance [24] [25]. Synthesizing all these effects leads to an additive random Gaussian error on the array weight vector [26]. In this work, we also study the performance degradation (POD and capacity) caused by these perturbation effects.

The paper is organized as follows: Section II introduces the WLPS structure. Section III discusses the theoretical analysis of the system performance for different system configurations as well as the perturbation effect. Section IV represents the simulation and analytical results. Section V concludes the paper. A table of abbreviations used throughout this paper is provided in Table I.

TABLE I
TABLE OF ABBREVIATIONS

BF	Beamforming
DBS	Dynamic Base Station
DOA	Direction of Arrival
DS-CDMA	Direct Sequence Code Division Multiple Access
GPS	Global Positioning System
IDR	ID Request Signal
IRT	ID Request Repetition Time
LPS	Local Positioning System
POD	Probability-of-Detection
SDMA	Spatial Division Multiple Access
TOA	Time Of Arrival
TRX	Transponder
WLPS	Wireless Local Positioning System

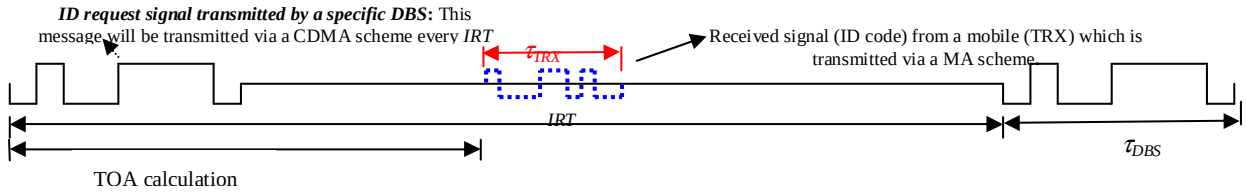

Fig. 1. Transmission of IDR and reception from TRX in DBS. Assuming a Pseudo Random ID codes, the number of the bits in the code represents the maximum capacity of the WLPS.

II. WLPS STRUCTURE

The two WLPS main parts include: A dynamic base station (DBS) and a transponder (TRX). The DBS transmitter generates an ID code request (IDR) signal every IRT (ID request repetition time) to all TRXs in the coverage area; then, it waits to receive a response back from the TRX within IRT (see Fig. 1). TRX transmits a unique ID code as soon as it detects the IDR signal transmitted by the DBS. The ID code is selected from simple pseudo random codes which consist of +1 and -1. Hence, the number of bits in the code depicts the maximum capacity of the WLPS. Depending on the application, the ID code can be assigned permanently or can be assigned by the DBS transmitter. The structure of DBS is shown in Fig. 2.

In a WLPS structure, each DBS communicates with a number of TRX in its coverage area

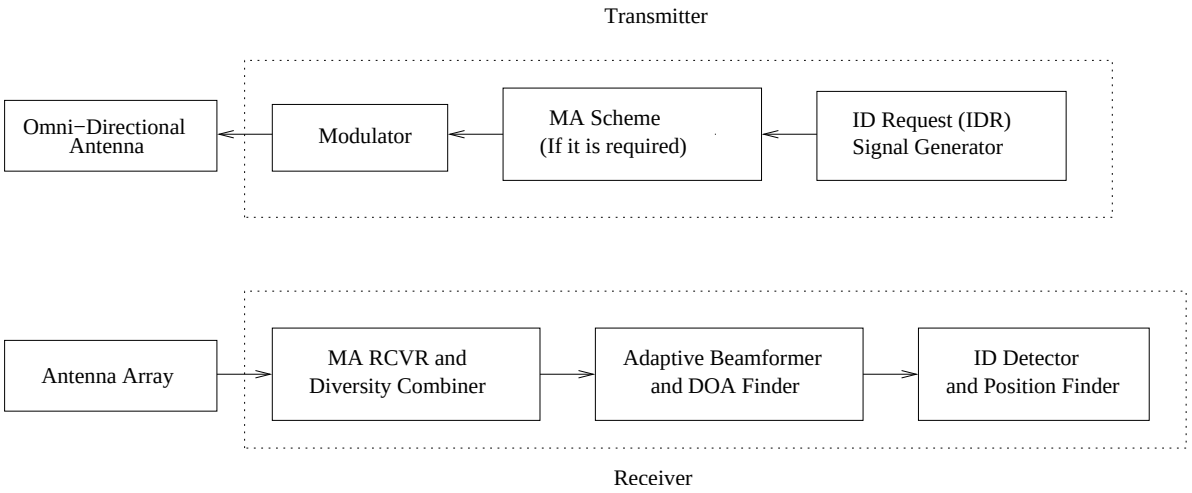

Fig. 2. DBS structure

simultaneously. This is the same as usual cellular communication systems. However, in contrast to cellular systems, in WLSP each TRX communicates with a number of DBS simultaneously as well. In addition, the time of transmission and reception would be different at the DBS, as shown in Fig. 1. Moreover, the whole DBS and TRX use different transmission frequencies. Thus, the overall system is considered as a time division duplex (TDD)-frequency division duplex (FDD), that is, hybrid TDD/FDD communication system (differ from cellular systems that are either TDD or FDD). This allows WLPS to reduce the interference effects via a proper selection of IRT.

The minimum allowable value for IRT (IRT_{min}) is calculated to avoid range ambiguity: If the response to each IDR signal is received in DBS within IRT, mobile range is calculated correctly; however, if it is received after the next IDR transmission, the range is not correctly calculated. Here, IRT is a function of the maximum coverage or the maximum range R_{max}. The minimum allowable IRT corresponds to:

$$IRT_{min} = 2T_{max} + T_d + T_G, \tag{1}$$

where T_{max} denotes the maximum possible time delay between the TRX transmission and the DBS reception, T_d is the TRX time delay in responding to the IDR signal which determines

the minimum time before receiving the first signal back from a TRX, and T_G is the guard band time to avoid range ambiguity, corresponds to [27]:

$$T_G = 5T_m + \tau_{DBS} + \tau_{TRX}. \tag{2}$$

Here, T_m is the wireless channel delay spread, τ_{DBS} and τ_{TRX} are the durations of DBS and TRX transmitted signals, respectively. Considering the maximum uplink antenna array half power beam widths (HPBW) β to be less than 90°, using a simple geometry in a scattering environment, T_{max} is determined by R_{max} and β via [27]:

$$T_{max} = \left(\frac{R_{max}}{2c}\right) \cdot \frac{1+\cos\beta}{\cos\beta}, \tag{3}$$

where c denotes the speed of light. Eq. (1) refers to a lower limit for IRT (i.e., IRT_{min}). The upper limit for IRT (IRT_{max}) is a function of the speed of moving TRX and DBS, and accordingly, the required processing speed.

The TRX receiver is subject to inter-DBS interference (IBI), since more than one DBS may transmit IDR signals in the coverage area of a TRX. Large selection of IRT reduces the probability-of-overlap, p_{ovl}, or collision of the DBSs transmitted signals at the TRX receiver. In addition, a number of TRXs in the DBS coverage area respond to the IDR signal of one DBS simultaneously, causing inter-TRX-interference (IXI) at the DBS receiver. Both IXI and IBI are functions of the p_{ovl} for the transmitted signals from TRXs and DBSs, respectively. p_{ovl} has a profound effect on the performance of the receiver, is a function of the number of mobiles or transmitters (DBS or TRX), K, in their coverage area, and corresponds to:

$$p_{ovl} = 1 - (1 - d_c)^{K-1}, \tag{4}$$

where $d_c = \tau/T$, $\tau = \tau_{DBS}(\tau_{TRX})$ is the duration of DBS (TRX) transmitted signal, and $T = T_{DBS}(T_{TRX})$, where $T_{DBS} = IRT_{min}$, $T_{TRX} = IRT$. Fig. 3 represents this probability as a function of the number-of-transmitters (TRX or DBS) for different values of duty cycle.

In general, large selection of IRT reduces IBI effects at the TRX receiver and highly enhances

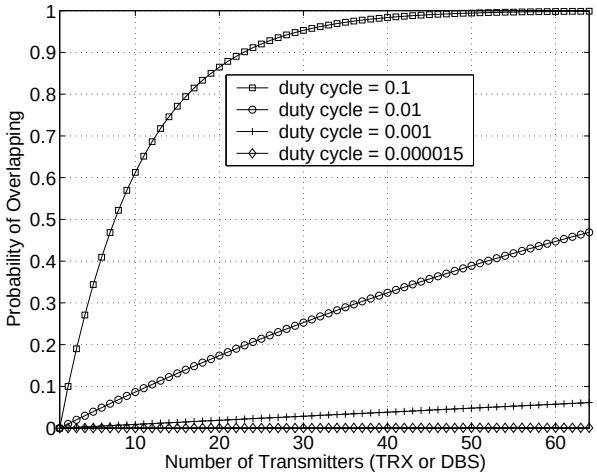

Fig. 3. The probability of overlapping.

its POD performance. However, the large selection of IRT does not affect the IXI, since all of the signals are received by DBS receiver within the T_{max} time frame, which is mainly a function of the maximum coverage range. It is also worth mentioning, each TRX located in the coverage area of more than one DBS may generate ID codes in response to more than one DBS within each IRT. This leads to both IXI as well as range ambiguity. Range ambiguity can be resolved via changing code assignments (MA codes, ID codes or both) for different DBS. In addition, in Eq. (4), the parameter d_c is a function of τ_{TRX} and τ_{DBS}, so as the probability-of-overlap and the POD performance of WLPS.

In general, selection of τ_{DBS} and τ_{TRX} depends on the POD, desired system capacity (in terms of the number of TRX/DBS accommodated), bandwidth, positioning accuracy and maximum coverage range, and may vary with WLPS application. The duration of the transmitted signal by the DBS (τ_{DBS}) and TRX (τ_{TRX}) should be much smaller than the IRT to reduce p_{ovl} among signals received by receivers of TRX and DBS, respectively. A smaller p_{ovl} decreases both the IBI effects (at TRX) and IXI effects (at DBS), which in turn enhances the POD performance and the capacity of the WLPS system. On the other hand, the system maximum capacity expressed by the maximum number of TRX (DBS) determines the number of bits within each ID code, which is to be transmitted over a period of τ_{TRX} (τ_{DBS}) . The required bandwidth is inversely

proportional to τ_{TRX} and τ_{DBS} for a given capacity. A large selection of IRT allows τ_{DBS} to be selected much larger than τ_{TRX} without sacrificing p_{ovl} at the TRX receiver. Hence, WLPS bandwidth is mainly determined by the value of τ_{TRX} (see Section IV, the simulation results).

III. WLPS Implementation And Theoretical Analysis

As discussed in Section II, in general, the interference effect IXI (IBI) at the DBS (TRX) receiver can be mitigated via selecting d_c small enough. Large selection of IRT reduces the d_c and consequently the IBI at the TRX receiver; however, large selection of IRT does not have any effect on the IXI at the DBS receiver. The d_c can also be reduced via small selection of τ (τ_{DBS} or τ_{TRX}), that in turn enhances the required bandwidth. Hence, while a standard receiver ensures TRX high performance for a multi-user environment, the DBS performance is improved just via MA schemes. We start with the theoretical investigation of performance for standard receivers and then we continue the discussion for DS-CDMA schemes. The theoretical results discussed here can be equivalently applied to both TRX and DBS receivers.

A. Standard Receiver System

Assuming a standard receiver at the DBS (TRX), the transmitted signal from the TRX (DBS) corresponds to (see Fig. 1):

$$s^k(t) = g_\tau(t) \cdot \sum_{n=0}^{N-1} b^k[n] \cdot g_{T_b}(t - nT_b) \cdot \cos(2\pi f_c t), \tag{5}$$

where N denotes the number of bit per ID code (that represents the maximum capacity of the WLPS), $b^k[n]$ denotes the n^{th} bit of user k's ID, $T_b = \tau/N$ represents the DBS(TRX) bit duration where $\tau = \tau_{TRX}(\tau_{DBS})$; $g_\tau(t)$ and $g_{T_b}(t)$ are rectangular pulses with the duration τ and T_b, respectively.

Assuming a frequency selective channel, the received signal $r(t)$ at the DBS(TRX) receiver is a mixture of signals from different TRXs(DBSs) and different paths, which is given by:

$$r(t) = \sum_{k=1}^{K} \sum_{l=0}^{L^k-1} \sum_{n=0}^{N-1} \alpha_l^k b^k[n] \cdot g_{T_b}(t - \tau_l^k - nT_b) \cdot g_\tau(t - \tau_l^k) \cdot \cos(2\pi f_c t + \phi_l^k) + n(t), \tag{6}$$

where K denotes the total number of TRXs(DBSs), L^k is the number of paths for TRX(DBS) k, and α_l^k, τ_l^k, ϕ_l^k denote the fading factor, time delay and random phase for k^{th} user's l^{th} path, respectively.

After the demodulation, the n^{th} bit output for j^{th} DBS's (TRX's) q^{th} path corresponds to:

$$y_q^j[n] = \int_{\tau_q^j+nT_b}^{\tau_q^j+(n+1)T_b} r(t)\cos(2\pi f_c t + \phi_q^j)\,dt, \tag{7}$$

Assuming all TRXs(DBSs) have the same number of paths, i.e., $L^k = L, \forall k$, and fading energy is uniformly distributed in paths, i.e., $E[(\alpha_q^j)^2] = 1/L$, the instantaneous SINR in j^{th} user's q^{th} path, i.e., for any path of any TRX(DBS) is:

$$r_i = \frac{A_a}{D_a \cdot (K-1) + D_a \cdot (1-\frac{1}{L}) + \frac{1}{\bar{r}_0}} \cdot \frac{1}{2L}, \tag{8}$$

where $\bar{r}_0$ is the average SNR, which is defined as the ratio between average bit energy and white noise. In this case,$A_a = 1$, $D_a = d_c$, and d_c denotes the duty cycle [see Eq. (4)].

B. Standard Receiver merger with Antenna Arrays and Conventional Beamforming (BF)

BF techniques reduce the signal from other users and other paths as long as they are in different direction from the desired user and path. In this case, with the same transmitted signal as Eq. (5), the received signal at the DBS(TRX) with antenna arrays corresponds to:

$$\vec{r}(t) = \sum_{k=1}^{K}\sum_{l=0}^{L^k-1}\sum_{n=0}^{N-1} \alpha_l^k \cdot \vec{V}(\theta_l^k) \cdot b^k[n] \cdot g_{T_b}(t-\tau_l^k-nT_b) \cdot g_\tau(t-\tau_l^k) \cdot \cos(2\pi f_c t + \phi_l^k) + \vec{n}(t), \tag{9}$$

where $\vec{V}(\theta_l^k)$ denotes the array response vector and corresponds to:

$$\vec{V}(\theta_l^k) = \left[1 \quad exp(j \cdot \frac{-2\pi d\cos(\theta_l^k)}{\lambda}) \quad \cdots \quad exp(j \cdot \frac{-2(M-1)\pi d\cos(\theta_l^k)}{\lambda})\right]^T. \tag{10}$$

Here, d is the spacing between antenna elements, M is the total number of antennas, λ denotes the carrier wavelength and θ_l^k is the direction of k^{th} user's l^{th} path.

After BF and demodulation, the n^{th} bit for j^{th} user's q^{th} path corresponds to:

$$y_q^j[n] = \vec{W}^H(\theta_q^j) \int_{\tau_q^j+nT_b}^{\tau_q^j+(n+1)T_b} \vec{r}(t)\cos(2\pi f_c t + \phi_q^j)\,dt, \tag{11}$$

where $\vec{W}(\theta_q^j) = \vec{v}(\theta_q^j)$ if no perturbation presents, and H denotes Hermition transpose. $\vec{W}(\theta_q^j)$ with perturbation is explained in subsection III-E.

In this case, the SINR for any path of any user is:

$$r_i = \frac{A_b}{B_b \cdot D_b \cdot (K-1) + B_b \cdot D_b \cdot (1-\frac{1}{L}) + \frac{M}{\bar{r}_0}} \cdot \frac{1}{2L}, \tag{12}$$

where $A_b = M^2$, $D_b = d_c$, and

$$B_b = \sum_{m=0}^{M-1}(m+1)J_0(\frac{2\pi dm}{\lambda})J_0(\frac{-2\pi dm}{\lambda}) + \sum_{m=M}^{2M-2}(2M-m-1)J_0(\frac{2\pi dm}{\lambda})J_0(\frac{-2\pi dm}{\lambda}). \tag{13}$$

Here, J_0 represents the zeorth order Bessel function of the first kind.

C. The DS-CDMA System

The transmitted DS-CDMA signal by the k^{th} TRX (DBS) corresponds to:

$$s^k(t) = g_\tau(t) \cdot \sum_{n=0}^{N-1} b^k[n] \cdot g_{T_b}(t-nT_b) \cdot a^k(t-nT_b) \cdot \cos(2\pi f_c t), \tag{14}$$

where $a^k(t) = \sum_{i=0}^{G-1} C_i^k g_{T_c}(t-iT_c)$, $C_i^k \in \{-1, 1\}$, denotes the spreading code, and G is the processing gain (code length), $T_c = \tau/(N \cdot G)$, $\tau = \tau_{TRX}(\tau_{DBS})$, represents the chip duration and, $g_{T_c}(t)$ is a rectangular pulse with the duration of T_c.

The received signal corresponds to:

$$r(t) = \sum_{k=1}^{K}\sum_{l=0}^{L^k-1}\sum_{n=0}^{N-1} \alpha_l^k b^k[n] \cdot g_{T_b}(t-\tau_l^k-nT_b) \cdot g_\tau(t-\tau_l^k) \cdot a^k(t-\tau_l^k-nT_b) \cdot \cos(2\pi f_c t+\phi_l^k) + n(t). \tag{15}$$

After despreading, the n^{th} bit output of j^{th} DBS's(TRX's) q^{th} path corresponds to:

$$y_q^j[n] = \int_{\tau_q^j+nT_b}^{\tau_q^j+(n+1)T_b} r(t) \cdot \cos(2\pi f_c t + \phi_q^j) \cdot a^k(t-\tau_q^j-nT_b)\,dt. \tag{16}$$

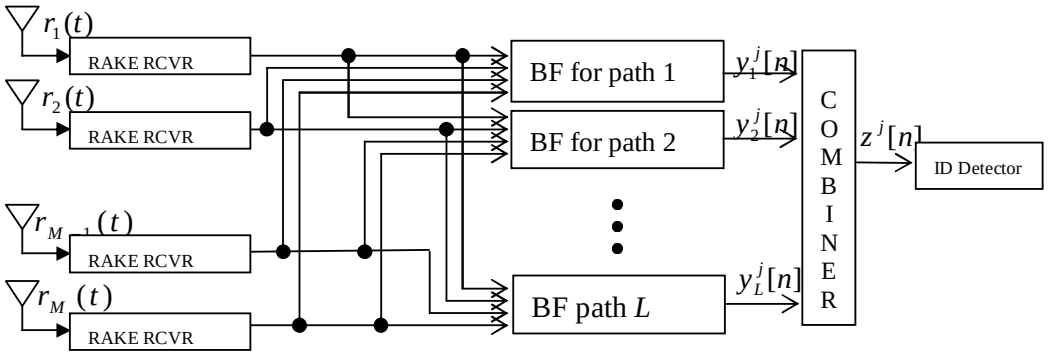

Fig. 4. DBS(TRX) receiver structure assuming a frequency selective channel and smart antennas with DS-CDMA

Finally the SINR for any path of any DBS(TRX) is:

$$r_i = \frac{A_c}{D_c \cdot (K-1) + D_c \cdot (1 - \frac{1}{L}) + \frac{G}{\bar{r}_0}} \cdot \frac{1}{2L}, \tag{17}$$

where $A_c = G$, and

$$D_c = d_c - \frac{N^2 - 3N + 3}{2N^2} \cdot d_c^2. \tag{18}$$

D. DS-CDMA Merger with SDMA (antenna array with conventional BF)

With the same transmitted signal as in Eq. (14), the received signal at the DBS (TRX) for the antenna array (see Fig. 4), which is a mixture of signals from different TRXs(DBSs) and different paths, is given as:

$$\vec{r}(t) = \sum_{k=1}^{K} \sum_{l=0}^{L^k-1} \sum_{n=0}^{N-1} \alpha_l^k \cdot \vec{V}(\theta_l^k) \cdot b^k[n] \cdot g_{T_b}(t - \tau_l^k - nT_b) \cdot g_\tau(t - \tau_l^k) \cdot a^k(t - \tau_l^k - nT_b) \cdot \cos(2\pi f_c t + \phi_l^k) + \vec{n}(t). \tag{19}$$

The i^{th} bit output of BF for j^{th} user's q^{th} path is given as:

$$y_q^j[n] = \vec{W}^H(\theta_q^j) \int_{\tau_q^j + nT_b}^{\tau_q^j + (n+1)T_b} \vec{r}(t) \cdot \cos(2\pi f_c t + \phi_q^j) \cdot a^k(t - \tau_q^j - nT_b)\, dt. \tag{20}$$

Finally, the SINR for any path of any user corresponds to:

$$r_i = \frac{A_d}{B_d \cdot D_d \cdot (K-1) + B_d \cdot D_d \cdot (1 - \frac{1}{L}) + \frac{MG}{\bar{r}_0}} \cdot \frac{1}{2L}, \tag{21}$$

where $A_d = M^2 G$, $B_d = B_b$, and $D_d = D_c$.

E. Perturbation effects

Here, we investigate the effects of perturbation in sensor position, channel phase estimation, and the effects of mutual coupling between sensors, receiver fluctuation due to temperature and humidity, quantization effects, different cable length for each sensor, imperfect channel phase estimation, etc. According to Central Limit Theorem, the summation of these effects leads to additive zero mean Gaussian random variables along the elements in the array, i.e., the weighting vector $\vec{W}(\theta_l^k)$ in Eq. (16) and (20) does not match array response vector $\vec{V}(\theta_l^k)$ exactly, but corresponds to $\vec{W}(\theta_l^k) = \vec{V}(\theta_l^k) + \vec{E}$, where $\vec{E}$, called error vector, denotes a column vector that contains M independent Gaussian random variables with zero mean and variance σ_ϵ^2 [28].

With this error vector, the peak of the directional beam does not point to the desired user perfectly, but steered away from the desired user. Therefore, the power of the desired user is reduced. In addition, sidelobe's power of the directional beam increases; hence, power of IXI(IBI) increases. As a result, SINR is reduced by perturbation, which is a function of σ_ϵ^2.

With perturbations, for standard receiver with antenna arrays, as introduced in Eq. (12), the SINR for any path of DBS(TRX) corresponds to:

$$r_i = \frac{A_e}{B_e \cdot D_e \cdot \frac{(K-1)}{2} + B_e \cdot D_e \cdot (1 - \frac{1}{L}) + \frac{M+\sigma_\epsilon^2}{2\bar{r}_0}} \cdot \frac{1}{L},$$

where $D_e = d_c$,

$$A_e = M^2 + \sigma_\epsilon^2 \sum_{m=0}^{M-1} J_0(2 \cdot \frac{2\pi dm}{2}), \tag{22}$$

$$B_e = \sum_{m=0}^{M-1} (m+1) J_0(\frac{2\pi dm}{\lambda}) J_0(\frac{-2\pi dm}{\lambda}) + \sum_{m=M}^{2M-2} (2M-m-1) J_0(\frac{2\pi dm}{\lambda}) J_0(\frac{-2\pi dm}{\lambda}) + \sigma_\epsilon^2 \sum_{m=0}^{M-1} J_0(2 \cdot \frac{2\pi dm}{2}). \tag{23}$$

Similarly, for DS-CDMA system with antenna arrays, as introduced in Eq. (21), the SINR for any path of any user corresponds to:

$$r_i = \frac{A_f}{B_f \cdot D_f \cdot \frac{(K-1)}{2} + B_f \cdot D_f \cdot (1 - \frac{1}{L}) + \frac{(M+\sigma_\epsilon^2) \cdot G}{2\bar{r}_0}} \cdot \frac{1}{L},$$

where $D_f = D_e$, $B_f = B_e$ as introduced in Eq. (23), and

$$A_f = G \cdot (M^2 + \sigma_\epsilon^2 \sum_{m=0}^{M-1} J_0(2 \cdot \frac{2\pi dm}{2})). \tag{24}$$

F. Path Diversity Combining

Finally, for all of the receivers discussed in parts A-E, we apply Maximal Ratio Combining (MRC) across the path diversity components [29]:

$$z^j[n] = \sum_{l=1}^{L} \alpha_l^j y_l^j[n]. \tag{25}$$

Therefore, the final instantaneous SINR expression can be written as:

$$r_0 = r_e \cdot (\alpha_1^2 + \alpha_2^2 + \cdots + \alpha_L^2). \tag{26}$$

In Eq. (26), the parameter r_e has been defined in Eq. (8), (12), (17), (21), corresponding to the receivers introduced in previous subsections. The Bit-Error-Rate for all of the discussed receivers corresponds to:

$$P_e = \int_0^\infty Q(\sqrt{2r_0}) f(r_0|\bar{r}_0)\, dr_0 = 0.5 \left(1 - \sqrt{\frac{r_e}{L + r_e}} \cdot \sum_{l=0}^{L-1} \binom{2l}{l} \cdot \frac{L^l}{2^{2l} \cdot (L + r_e)^l} \right). \tag{27}$$

For frequency-selective channel, L is greater than one. For flat-fading channel, L equals to one. If all bits are detected correctly, the ID of the desired user is detected correctly. Therefore, the probability-of-detection is given as:

$$P_d = (1 - P_e)^N, \tag{28}$$

and the probability-of-miss-detection corresponds to:

$$P_{md} = 1 - P_d. \tag{29}$$

IV. Numerical Results And Analysis

In this section, we evaluate the POD performance and capacity (in terms of number-of-TRXs(DBSs)) of WLPS system under multi-TRX, multi-path environment, via simulations and we compare the results with the theoretical result of Eq. (28). This setup is typically useful for vehicle collision avoidance applications, where each vehicle is required to cover the front area. For simulation purposes, we assume:

1) The ID code has 6 bits ($N = 6$);
2) The DS-CDMA code has 64 chips ($G = 64$);
3) Channel delay spread, T_m for a typical street area is $27\,nsec$ [30];
4) Carrier frequency = $3\,GHz$, $\tau_{TRX} = 1.2\,\mu s$, and $\tau_{DBS} = 24\,\mu s$;
5) The antenna array is linear with 4 elements, and element spacing $d = \frac{\lambda}{2} = 0.05\,m$ ($HPBW = 27°$);
6) Four multipaths lead to $L = 4$ fold path diversity for DS-CDMA system;
7) The TRX distance and angle are uniformly distributed in $[\,0 \quad 1\,]\,km$ and $[\,0 \quad \pi\,]$, respectively;
8) Uniform multi-path intensity profile, i.e., bit energy is distributed in each path identically;
9) Binary Phase Shift Keying (BPSK) modulation;
10) Perfect power control and DOA, TOA estimation; and,
11) The average Signal-to-Noise Ratio (SNR) introduced in Eq. (8), (12), (17) and (21) is $\bar{r}_0 = 20\,dB$.
12) The error variance, if perturbation presents, equals to 0.5, i.e., $\sigma_\epsilon^2 = 0.5$. This error variance means the standard deviation of perturbations is around 70% of elements of array response vector without perturbations.

Based on the assumed setup, then we deduce that TRX signal TOA is uniformly distributed in $[\,T_d \quad T_{max}\,]$, at the DBS receiver. Assuming $T_d \ll T_{max}$, the TRX signal TOA is approximately

uniformly distributed in $[\,0 \quad T_{max}\,]$. In addition, the minimum IRT, IRT_{min}, is $32\,\mu sec$ [c.f., Eq. (1)]. We select a larger value $IRT = 24\,msec$ in order to reduce the IBI effects. It is worth mentioning that in the assumptions, τ_{DBS} is selected larger than τ_{TRX}, since the IBI effect at the TRX receiver can be removed via large selection of IRT. Hence, a smaller bandwidth is required for the DBS transmitter. With the assumed τ_{DBS} and τ_{TRX}, the required bandwidth of a DS-CDMA (standard) transmitter is $320MHz$ ($5MHz$) for TRX, and $16MHz$ ($250KHz$) for DBS, respectively. Hence, DBS required bandwidth is much smaller than the TRX and the WLPS bandwidth is mainly determined by the TRX transmission bandwidth, as expected. In addition, using these parameters, the duty cycle for DBS and TRX receivers correspond to $d_{c,DBS} \simeq 0.1$ and $d_{c,TRX} \simeq 0.001$. Fig. 3 depicts p_{ovl} as a function of the number of transmitters (TRX or DBS) for various values of the duty cycle that is a function of IRT.

As we mentioned earlier, the IBI at the TRX receiver can be considerably reduced by selecting the IRT as large as possible; however, this selection will not affect IXI at the DBS receiver. Hence, a TRX receiver can just be implemented by a simple transceiver (or DS-CDMA) system without employment of BF, while a DBS receiver needs a combination with BF. It should be mentioned that antenna arrays are required at the DBS receiver for DOA estimation as well. A small $d_{c,TRX} \simeq 0.001$ at the TRX receiver leads to a small p_{ovl}, which leads to small IBI and high POD. In contrast, a large $d_{c,DBS} \simeq 0.1$ at the DBS receiver leads to a high p_{ovl} that results in high IXI. Both BF and CDMA techniques help to reduce the IXI effects at DBS.

The POD (P_d) of the DBS receiver is depicted in Fig. 5. This figure compares P_d vs. the number of TRX for a standard transceiver and a DS-CDMA transceiver, with or without antenna arrays. It shows that in general the P_d decreases as the number of TRX increases, which is a direct result of IXI. While beamforming enhances the POD for a standard receiver, yet it does not lead to a high POD performance (see the lower two curves). However, BF considerably enhances the capacity of the DS-CDMA system (see the 3^{rd} and 6^{th} curves from the bottom). Merging DS-CDMA with BF is thus highly promising for enhancing the P_d performance of WLPS systems. In Fig. 5 the solid lines represent the theoretical results which have a good match with the simulations.

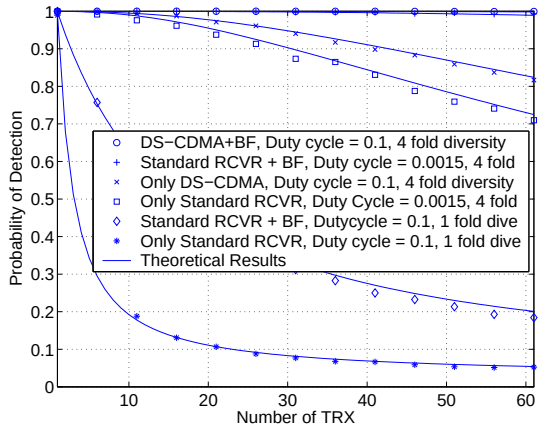

Fig. 5. Simulation results for DBS receivers, without perturbation.

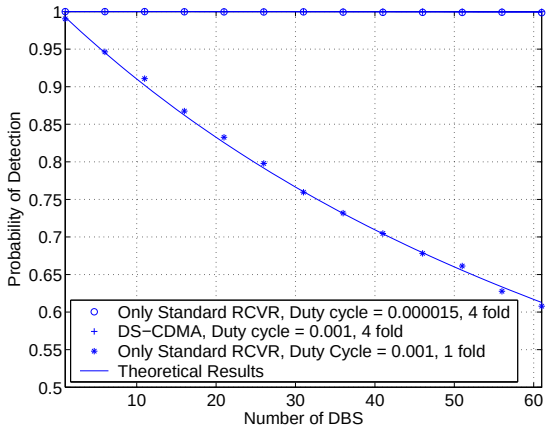

Fig. 6. Simulation results for TRX receivers, without perturbation.

The P_d results for TRX receiver using standard receiver is shown in Fig. 6. Although simple, a standard TRX receiver typically achieves good P_d performance. Further improvement is possible by selecting a larger IRT value, or a smaller τ_{DBS} value. Occupying the same bandwidth as DS-CDMA, a standard receiver should choose τ_{TRX} (τ_{DBS}) to be $1/64^{th}$ of that of a DS-CDMA system. In this case, the same number of path diversity as the DS-CDMA receiver (i.e., four fold diversity) is achievable. This corresponds to $d_{c,TRX} \simeq 0.000015$ ($d_{c,DBS} \simeq 0.0015$), which leads to a very small p_{ovl} at the DBS (TRX) receiver and very high P_d. This fact has been shown in Fig. 5 (see 5^{th} curve from the bottom) and Fig. 6 (see the top curves). The top curves in Fig. 5 and Fig. 6 have been redrawn in Fig. 7 and 9. In addition, the probability-of-miss-detection

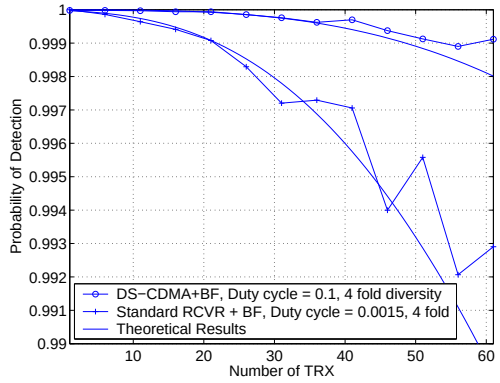

Fig. 7. The top two curves of Fig. 5: Probability of Detection.

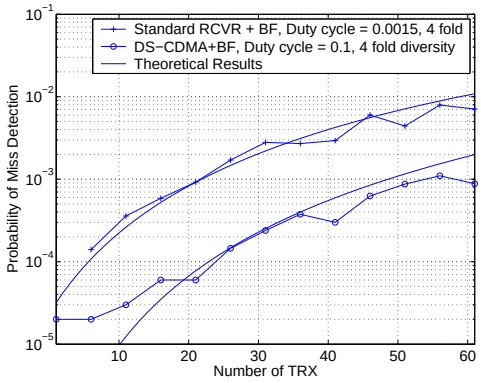

Fig. 8. Probability of miss Detection corresponds to Fig. 7.

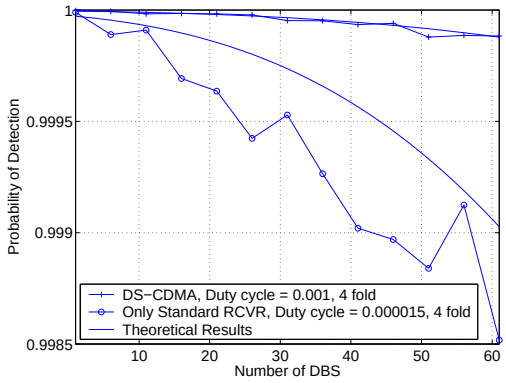

Fig. 9. The top two curves of Fig. 6: Probability of Detection.

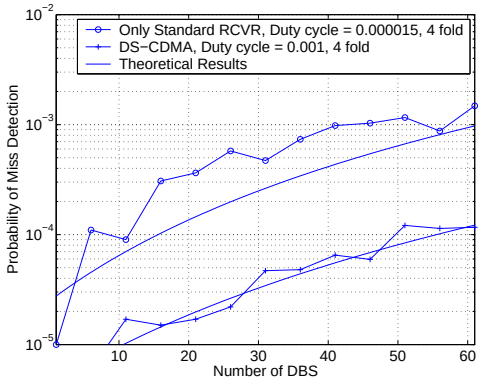

Fig. 10. Probability of miss Detection corresponds to Fig. 9.

[defined in Eq. (29)] corresponding to the curves in Fig. 7 and 9 have been sketched in Fig. 8 and 10, respectively.

Fig. 7 and 8 show that, at the DBS receiver with similar bandwidths, DS-CDMA receivers outperforms standard receivers. When high number of TRXs are available, (e.g., Number of TRX=60), P_d of standard system is approximately 99%, while P_d of DS-CDMA system is approximately 99.8%. Hence, P_d of DS-CDMA system satisfies most tracking purposes, which is due to a combination of path diversity and orthogonality achieved via these systems.

Fig. 10 shows that, at the TRX receiver with similar bandwidths, a DS-CDMA system outperforms standard system too. Because of the large selection of IRT helps reduce IBI, TRX receiver with antenna array performance is even better than DBS receiver with antenna array in

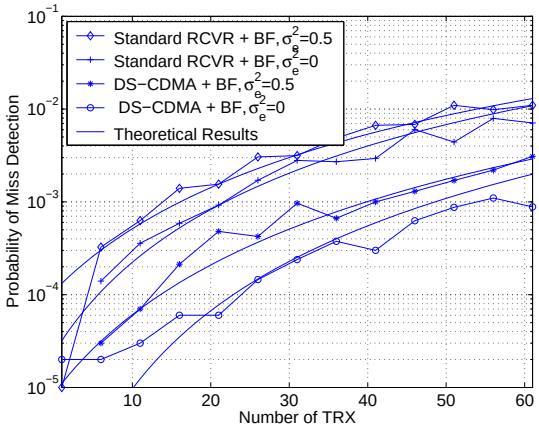

Fig. 11. DBS performance with perturbations vs. Number of Users.

similar environments. When high number of TRXs are available,(e.g., Number of TRX=60), P_d of standard system is approximately 99.9%, while P_d of DS-CDMA system is approximately 99.99%. Note that the TRX receiver performance can also be improved via larger selection of IRT (such as $0.24\,sec$). Due to simplicity, a standard receiver system is recommended for TRX receiver.

Fig. 11 shows the capacity of the system, i.e., the probability-of-miss-detection as a function of the number of TRX, under perturbations. This figure shows the system capacity decreases as the error variance equals to 0.5, and setting the probability-of-miss-detection threshold at 0.1%, the system capacity is reduced by 20% for DS-CDMA system, and 30% for standard systems.

V. CONCLUSIONS

This paper presents a novel WLPS system. With a DBS/TRX structure and a novel signaling technique, WLPS would have various applications in road safety (vehicle collision avoidance), multirobot control, defense, law enforcement, and security. We studied and compared the probability-of-detection (POD) performance and the capacity of DBS and TRX with both DS-CDMA and standard systems with and without beamforming (BF) for a special setup suitable for road safety applications. The study shows that with similar bandwidth both DS-CDMA and standard systems with BF ensures high POD performance and capacity while DS-CDMA

technique leads to a better performance comparing to standard receivers. We also investigated the perturbation effects in DBS antenna array weights. Perturbation reduces the asymptotic system POD performance and capacity. Future studies will focus on the development of unique DOA estimation for WLPS as well as adaptive BF techniques at the DBS receiver for high scattering environments.

REFERENCES

[1] S. A. Zekavat, "Mobile Base Station (MBS) wireless with applications in vehicle early warning systems," in *Proceedings the University of Texas at Austin 2003 Wireless Networking Symposium*, Oct. 2003.

[2] S. A. Zekavat, H. Tong, and J. Tan, "A Novel Wireless Local Positioning System for Airport (Indoor) Security," in *Proceedings of The International Society for Optical Engineering (SPIE 2004)*.

[3] H. Tong and S. A. Zekavat, "LCMV Beamforming for a Novel Wireless Local Positioning System: A Stationarity Analysis," in *Proceedings of The International Society for Optical Engineering (SPIE 2005)*, Mar. 2005.

[4] L. V. Grant, "An overview of the Federal Radionavigation Plan," in *IEEE 21st Annual conference on Electronics and Aerospace Conference, (EASCON'88)*, Nov. 1988, pp. 173–177.

[5] I. A. Getting, "Perspective/Navigation-The Global Positioning System," *IEEE Spectrum*, vol. 30, no. 12, pp. 36–38, Dec. 1993.

[6] J. Werb and C. Lanzl, "Designing a positioning system for finding things and people indoors," *IEEE Spectrum*, vol. 35, no. 9, pp. 71–78, Sept. 1998.

[7] M. E. Bernard, "The Global Positioning System," *IEE Review*, vol. 38, pp. 99–102, Mar. 1992.

[8] M. Vossiek, L. Wiebking, P. Gulden, J. Wieghardt, and C. Hoffmann, "Wireless local positioning - Concepts, solutions, applications," in *Radio and Wireless Conference, RAWCON '03. Proceedings*, Aug. 2003, pp. 219–224.

[9] M. I. Skolnik, *Introduction to Radar Systems*. Mc-Graw Hill Co, 1981.

[10] M. Sekine, T. Senoo, I. Morita, and H. Endo, "Design method for an automotive laser radar system and future prospects for laser radar," in *Intelligent Vehicles Symposium '92.*, 1992, pp. 120–125.

[11] R. Hermann, M. Marc-Michel, K. Michael, and L. Urs, "Research activities in automotive Radar," in *MSMW'01 Symp.*, 2001.

[12] K. Saneyoshi, "Drive assist system using stereo image recognition," in *IEEE Intelligent Vehicle Symp.*, 1996, pp. 230–235.

[13] T. Williamson and N. A. Spencer, "Development and operation of the Traffic Alert and Collision Avoidance System (TCAS)," *IEEE Control Systems Magazine*, vol. 77, no. 11, pp. 1735–1744, Nov. 1989.

[14] S. Kahne and I. Frolow, "Air traffic management: evolution with technology," *IEEE Proceedings*, vol. 16, no. 4, pp. 12–21, Aug. 1996.

[15] R. M. Trim, "Mode S: An introduction and overview [secondary surveillance radar]," *Journal of Electronics and Communication Engineering*, vol. 2, no. 2, pp. 53–59, Apr. 1990.

[16] S. Ractliffe, “Air traffic control and mid-air collisions,” *Journal of Electronics and Communication Engineering*, vol. 2, no. 5, pp. 202 – 208, Oct. 1990.

[17] M. Cedervall, “Mobile positioning for third generation WCDMA systems,” in *IEEE 1998 International Conference on Universal Personal Communications, (ICUPC ’98)*, Oct. 1998.

[18] E. Hepsaydir, “Analysis of mobile positioning measurements in CDMA cellular networks,” in *1999 IEEE Radio and Wireless Conference, (RAWCON ’99)*, Aug. 1999.

[19] S. Kikuchi, A. Sano, H. Tsuji, and R. Miura, “A novel approach to mobile-terminal positioning using single array antenna in urban environments,” in *2003 IEEE 58th Vehicular Technology Conference, VTC 2003-Fall*, vol. 2, Oct. 2003.

[20] L. M. Ni, Y. Liu, Y. C. Lau, and A. P. Patil, “LANDMARC: indoor location sensing using active RFID,” in *Proceedings of the First IEEE International Conference on Pervasive Computing and Communications, (PerCom ’2003)*, Mar. 2003.

[21] R. Singh, M. Guainazzo, and C. S. Regazzoni, “Location determination using WLAN in conjuction with GPS network (global positioning system),” in *2004 IEEE 59th Vehicular Technology Conference, VTC 2004-Spring*, May 2004.

[22] J. Li, J. Jannotti, S. J. Douglas, D. Couto, D. R. Karger, and R. Morris, “A Scalable Location Service for Geographic Ad Hoc Routing,” in *ACM Mobicom 2000*, Boston, MA, 2000, pp. 120–130.

[23] H. Gharavi and K. Ban, “Multihop sensor network design for wide-band communications,” *Proceedings of the IEEE*, vol. 91, no. 8, pp. 1221–1234, Aug 2003.

[24] J. Yang and A. L. Swindlehurst, “The effects of array calibration errors on DF-Based signal copy performance,” *IEEE Transactions on Signal Processing*, vol. 43, no. 11, pp. 2724–2732, Nov. 1995.

[25] L. C. Godara, “Application of antenna arrays to mobile communications. II. Beam-forming and direction-of-arrival considerations,” *Proceedings of the IEEE*, vol. 85, no. 8, pp. 1195–1245, Aug 1997.

[26] M. Wax and Y. Anu, “Performance analysis of the minimum variance beamformer in the presence of steering vector errors,” *IEEE Transactions on Signal Processing*, vol. 44, no. 4, pp. 938–947, Apr 1997.

[27] S. A. Zekavat, “A novel application for wireless communications in vehicle early warning,” in *Consumer Communications and Networking Conference*, Jan 2004, pp. 715–717.

[28] A. M. Rao and D. L. Jones, “Efficient quadratic detection in perturbed arrays via Fourier transform techniques,” *IEEE Transactions on Signal Processing*, vol. 49, no. 7, pp. 1269 – 1281, July 2001.

[29] A. Shah and A. Haimovich, “Performance analysis of maximal ratio combining and comparison with optimum combining for mobile radio communications with cochannel interference,” *IEEE Transactions on Vehicular Technology*, vol. 49, no. 4, pp. 1454–1463, Jul 2000.

[30] A. A. Arowojolu, A. M. D. Turkman, and J. D. Parsons, “Time dispersion in urban microcellular enviroments,” in *IEEE 44th Vehicular Technical Conference*, vol. 1, jun 1994, pp. 150–154.